Substrate Binding to the Peripheral Site of Acetylcholinesterase Initiates Enzymatic Catalysis. Substrate Inhibition Arises as a Secondary Effect†

Tivadar Szegletes,‡ William D. Mallender,‡ Patrick J. Thomas,§ and Terrone L. Rosenberry*,‡

Department of Pharmacology, Mayo Foundation for Medical Education and Research, Department of Research, Mayo Clinic Jacksonville, Jacksonville, Florida 32224, and Department of Pharmacology, Case Western Reserve University School of Medicine, Cleveland, Ohio 44120-4965

Received June 9, 1998; Revised Manuscript Received October 13, 1998

ABSTRACT: Two sites of ligand interaction in acetylcholinesterase (AChE) were first demonstrated in ligand binding studies and later confirmed by crystallography, site-specific mutagenesis, and molecular modeling: an acylation site at the base of the active site gorge and a peripheral site at its mouth. We recently introduced a steric blockade model which demonstrated how small peripheral site ligands such as propidium may inhibit substrate hydrolysis [Szegletes, T., Mallender, W. D., and Rosenberry, T. L. (1998) *Biochemistry 37*, 4206−4216]. In this model, the only effect of a bound peripheral site ligand is to decrease the association and dissociation rate constants for an acylation site ligand without altering the equilibrium constant for ligand binding to the acylation site. Here, we first provide evidence that not only rate constants for substrates but also dissociation rate constants for their hydrolysis products are decreased by bound peripheral site ligand. Previous reaction schemes for substrate hydrolysis by AChE were extended to include product dissociation steps, and acetylthiocholine hydrolysis rates in the presence of propidium under nonequilibrium conditions were simulated with assigned rate constants in the program SCoP. We next showed that cationic substrates such as acetylthiocholine and 7-acetoxy-*N*-methylquinolinium (M7A) bind to the peripheral site as well as to the acylation site. The neurotoxin fasciculin was used to report specifically on interactions at the peripheral site. Analysis of inhibition of fasciculin association rates by these substrates revealed K_S values of about 1 mM for the peripheral site binding of acetylthiocholine and 0.2 mM for the binding of M7A. The AChE reaction scheme was further extended to include substrate binding to the peripheral site as the initial step in the catalytic pathway. Simulations of the steric blockade model with this scheme were in reasonable agreement with observed substrate inhibition for acetylthiocholine and M7A and with mutual competitive inhibition in mixtures of acetylthiocholine and M7A. Substrate inhibition was explained by blockade of product dissociation when substrate is bound to the peripheral site. However, our analyses indicate that the primary physiologic role of the AChE peripheral site is to accelerate the hydrolysis of acetylcholine at low substrate concentrations.

The hydrolysis of the neurotransmitter acetylcholine by acetylcholinesterase (AChE)[1] is one of the most efficient enzyme catalytic reactions known (*1*). The basis of this high efficiency has been investigated with ligand binding studies interpreted in the context of the AChE three-dimensional structure determined by X-ray crystallography (*2*). The long and narrow active site gorge is about 20 Å deep and includes two sites of ligand interaction: an *acylation site* at the base of the gorge and a *peripheral site* at its mouth. In the acylation site, residue S200 (TcAChE sequence numbering) is acylated and deacylated during substrate turnover, H440 and E327 participate with S200 in a catalytic triad, and W84 binds to the trimethylammonium group of acetylcholine as acyl transfer to S200 is initiated. The peripheral site involves other residues including W279 (*3*−*8*). Ligands can bind selectively to either the acylation or the peripheral sites, and ternary complexes with distinct ligands bound to each site can form (*9*). Ligands that bind specifically to the peripheral site include the phenanthridinium derivative propidium and the fasciculins, a family of very similar snake venom neurotoxins comprised of 61-amino acid polypeptides (*7*, *8*, *10*, *11*).

Despite its prominence, the role of the peripheral site in the AChE catalytic pathway has remained obscure. From analysis of the effect of ionic strength on k_{cat}/K_{app}, we proposed several years ago that acetylthiocholine binding to the active site is controlled by a high net negative charge near the active site that can electrostatically attract cationic substrates and inhibitors (*12*). Molecular modeling calculations (*13*, *14*) from the three-dimensional structure support this notion by suggesting that the AChE catalytic subunit has a dipole moment aligned with the active site gorge that can accelerate association rate constants for cationic ligands. The extent of this acceleration, measured as a ratio of the

† This work was supported by Grant NS-16577 from the National Institutes of Health and by grants from the Muscular Dystrophy Association of America. W.D.M. was supported by a Kendall-Mayo Postdoctoral Fellowship.

* To whom correspondence should be addressed.

‡ Mayo Clinic Jacksonville.

§ Case Western Reserve University School of Medicine.

[1] Abbreviations: AChE, acetylcholinesterase; TcAChE, acetylcholinesterase from *Torpedo californica*; DTNB, 5,5′-dithiobis(2-nitrobenzoic acid); TMTFA, *m*-(*N*,*N*,*N*-trimethylammonio)trifluoroacetophenone; M7A, 7-acetoxy-*N*-methylquinolinium; M7H, 7-hydroxy-*N*-methylquinolinium.

10.1021/bi9813577 CCC: $18.00
Published on Web 12/12/1998

association rate constant at low ionic strength to that at high ionic strength, depends on the cationic ligand and the species of AChE, but it appears to be about a factor of 7.5 for the cation TMTFA with mouse AChE at zero ionic strength (*15*). However, mutation of up to seven negatively charged residues at or near the peripheral site on the gorge rim reduced this factor by less than 60% (*15*, *16*), indicating that the peripheral site makes only a modest contribution to the electrostatic field at the active site. A second possibility is that ligand binding to the peripheral site results in a conformational change that promotes catalysis. Many peripheral site ligands inhibit substrate hydrolysis, and AChE inhibition by propidium has been attributed entirely to a conformational change at the acylation site induced by the binding of propidium to the peripheral site (*17*). If substrate interacted with the peripheral site on entering the active site gorge, this interaction in principle could induce a conformational change that might promote substrate hydrolysis. However, we recently introduced a steric blockade model which demonstrated how small peripheral site ligands such as propidium may inhibit substrate hydrolysis without inducing a conformational change in the acylation site (*18*). This model includes the simple hypothesis that the only effect of a bound peripheral site ligand is to decrease the association and dissociation rate constants for an acylation site ligand without altering the equilibrium constant for ligand binding to the acylation site. This hypothesis was generally supported by our direct demonstration that bound propidium decreased the association and dissociation rate constants for the acylation site ligands huperzine A and TMTFA by factors of 10−400. Therefore, there is little evidence that the binding of substrates and other small ligands to the peripheral site induces a conformational change that is significant with respect to catalysis.

In this paper, we show that further examination of our steric blockade model leads directly to a proposed new role for the peripheral site, namely, the initial binding of substrate on the AChE catalytic pathway. A similar role has been suggested for a peripheral site in the closely related enzyme butyrylcholinesterase (*19*). The first step in clarifying this role in AChE was to analyze further the inhibition of substrate hydrolysis by peripheral site ligands. We conducted nonequilibrium simulations that accounted quantitatively for inhibition by peripheral site ligands at low substrate concentrations but diverged from experimental data at higher substrate concentrations (*18*). The discordance prompted us here to extend the model to include steric blockade of product dissociation as well as of substrate association and dissociation by a bound peripheral site ligand. The extended model not only brought the simulations into quantitative agreement with experimental data at all substrate concentrations but also suggested that substrate binding to the peripheral site could block product release and account for the well-known phenomenon of substrate inhibition with AChE. With a competition assay for fasciculin binding to quantify the affinity of substrates for the peripheral site, we then demonstrated a satisfactory correspondence of the simulated and observed substrate inhibition data. The complete model indicates that the peripheral site serves as an initial binding site for substrate entry to the acylation site and that this initial binding accelerates the rate constant (k_{cat}/K_{app}) for substrate hydrolysis at low substrate concentrations.

EXPERIMENTAL PROCEDURES

Materials. Human erythrocyte AChE was purified as outlined previously, and active site concentrations were determined by assuming 410 units/nmol (*20*, *21*). Propidium iodide was purchased from Calbiochem. M7H iodide and some stocks of M7A iodide were obtained from Molecular Probes, while other stocks of M7A iodide were synthesized by the Mayo Clinic Jacksonville Organic Synthesis Core Facility. Fasciculin was the fasciculin 2 form obtained from C. Cervenansky at the Instituto de Investigaciones Biologicas (Clemente Estable, Montevideo, Uruguay) (*22*).

Steady State Measurements of AChE-Catalyzed Substrate Hydrolysis. Hydrolysis rates v were measured at various substrate (S) concentrations in 1 mL assay solutions with buffer (20 mM sodium phosphate and 0.02% Triton X-100 at pH 7.0) at 25 °C. To maintain a constant ionic strength with protocols in which the acetylthiocholine concentration exceeded 1 mM, NaCl was added such that the sum of the acetylthiocholine and NaCl concentrations was 60 mM. Acetylthiocholine assay solutions included 0.33 mM DTNB, and hydrolysis was monitored by formation of the thiolate dianion of DTNB at 412 nm [$\Delta\epsilon_{412nm} = 14.15$ mM^{-1} cm^{-1} (*23*)] for 1−5 min on a Varian Cary 3A spectrophotometer (*24*). Hydrolysis of M7A was followed by formation of M7H at 406 nm ($\Delta\epsilon_{406nm} = 9.2$ mM^{-1} cm^{-1} at pH 7.0), and nonenzymatic hydrolysis rates were deducted (*25*, *26*).

At high concentrations of acetylthiocholine and M7A, v declined below the maximal hydrolysis rates observed at lower S concentrations. The dependence of v on [S] was fitted to the Haldane equation for substrate inhibition (*27*) as shown in eq 1.

$$v = \frac{V_{max}[S]}{[S]\left(1 + \frac{[S]}{K_{SS}}\right) + K_{app}} \quad (1)$$

In eq 1, $V_{max} = k_{cat}[E]_{tot}$ where $[E]_{tot}$ is the total concentration of AChE active sites. Data were fitted with Fig.P (BioSoft, version 6.0) to eq 1 by nonlinear regression analyses; with experimental data, weighting assumed that v has a constant percent error.

At low concentrations of acetylthiocholine and M7A, reciprocal plots of v^{-1} vs $[S]^{-1}$ were linear. Competitive inhibition constants (K_I) for inhibitors I were obtained by either (1) analysis of replots of reciprocal plot slopes obtained over a range of fixed concentrations of I (*18*) or (2) direct measurements of the second-order hydrolysis rate constants z in the presence and absence of I at low S concentrations. When I was a competing substrate, z was measured as an initial velocity at low S concentrations (i.e., $[S] < 0.1K_{app}$). The extent of acetylthiocholine hydrolysis in the presence of M7A was measured with 20 μM pyridine disulfide (2,2′-dithiobispyridine; Acros) in place of DTNB. Absorbance of pyridine thiol was monitored at 347 nm [$\Delta\epsilon_{341nm} = 8.1$ mM^{-1} cm^{-1} (*28*)] because 347 nm corresponded to the isosbestic point of M7H and M7A. The extent of M7A hydrolysis in the presence of acetylthiocholine was measured on a Perkin-Elmer LS 50B luminescence spectrometer [excitation at 400 nm, emission at 500 nm (*25*)]. When I was an inhibitor that

was not metabolized, z was determined as a pseudo-first-order rate constant from eq 2 (*22*).

$$[S] = [S]_0 e^{-zt} \quad (2)$$

Equation 2 is valid when the initial substrate concentration $[S]_0$ is low (i.e., $[S]_0 \ll K_{SS}$ and $[S]_0 <$ about $0.2K_{app}$). In the absence of I, z is denoted $z_{I=0} = V_{max}/K_{app}$ and eq 2 corresponds to the integrated form of eq 1. Measured z values at various I concentrations were fitted to eq 3 to obtain K_I and the constant α (*18*).

$$\frac{z}{z_{I=0}} = \frac{\left(1 + \frac{[I]}{K_I}\right)}{\left(1 + \frac{\alpha[I]}{K_I}\right)} \quad (3)$$

For inhibitors that bind to the peripheral site and form ternary complexes ESI_P (see Scheme 1 below), α is a measure of the acylation rate constant through the ternary complex at low substrate concentrations relative to k_{cat}/K_{app} (*18*). In contrast, for inhibitors that bind preferentially to the acylation site, α is essentially zero.

Slow Equilibration of Fasciculin in the Presence of Peripheral Site Inhibitors. The rates of fasciculin binding to the AChE peripheral site were analyzed by an extension of procedures used previously (*22*). Association reactions (2 mL) were initiated by adding small volumes of AChE and acetylthiocholine to final concentrations of 0.5−10 nM fasciculin and 0.1 mM DTNB in buffer (with [NaCl] = 60 mM − [S] as above) at 25 °C. Some reaction mixtures also included 20 μM propidium. The extent of fasciculin binding was measured under approximate first-order conditions in which the concentrations of all ligands were adjusted to at least 8 times the concentration of AChE and the acetylthiocholine level was not significantly depleted (<20%). Acetylthiocholine hydrolysis was monitored by continuous spectrophotometric assay as outlined above, and assay rates v over 2 s intervals were fitted by nonlinear regression analysis (Fig.P) to eq 4. In eq 4, $v_{initial}$ and v_{final} are the calculated values of v at time zero and at the final steady state when fasciculin binding has reached equilibrium, and k is the observed first-order rate constant for the approach to equilibrium.

$$v = v_{final} + (v_{initial} - v_{final})\, e^{-kt} \quad (4)$$

Each series of binding measurements included reactions at a fixed acetylthiocholine (S) concentration and at least four fasciculin concentrations [F]. The observed k for each reaction was given by eq 5, and k_{on}, the apparent association rate constant, was determined by weighted linear regression analysis in which k was assumed to have a constant percent error.

$$k = k_{on}[F] + k_{off} \quad (5)$$

If ligand binding to the peripheral site is unaffected by the presence of ligands or an acyl group at the acylation site, then only three sets of enzyme species need be considered: ΣE, ΣES_P, and ΣEI_P. These are the sums of the concentrations of all enzyme species in which nothing, S, or propidium (I), respectively, is bound to the peripheral site. Assuming that fasciculin (F) reacts only with species in ΣE and ΣES_P, k_{on} is given by eq 6.

$$k_{on} = \frac{k_F + k_{FP}\frac{[S]}{K_S}}{1 + \frac{[S]}{K_S} + \frac{[I]}{K_I}} \quad (6)$$

In eq 6, k_F is the intrinsic association rate constant for E and F, k_{FP} is the intrinsic association rate constant for ES_P and F, and K_S and K_I are the equilibrium dissociation constants for S and I, respectively, at the peripheral site. When eq 6 was employed, mean values of k_{on} obtained at each S concentration were fitted with Fig.P by nonlinear regression analysis with the reciprocals of the variances as weighting factors to give apparent K_S estimates. If ligand binding to the peripheral site is altered by the presence of a ligand at the acylation site, then k_{on} in eq 6 in principle must be extended by additional terms (*26*, *29*). We will assume that these additional terms can be grouped in ΣEX_A as shown in eq 7, where the specific terms in each sum are given in Scheme 5 in the Appendix and k_{FA} is the intrinsic association rate constant for species in ΣEX_A and F.

$$k_{on} = \frac{k_F([E] + [EA]) + k_{FP}\sum ES_P + k_{FA}\sum EX_A}{[E] + [EA] + \sum ES_P + \sum EX_A + \sum EI_P} \quad (7)$$

Equation 7 cannot be solved analytically, but it can be solved numerically with the SCoP simulation program as outlined in the text.

The value of K_S for M7A was obtained by a modification of the above procedure in which fasciculin association reactions were measured at 412 nm with 2 nM fasciculin, 0.25 mM acetylthiocholine, and 0−300 μM M7A in 1.0 mL of buffer without added NaCl. Observed k values were assumed to approximate k_{on}, and K_S was calculated from eq 6 (with [I] and k_{FP} set to 0).

Simulations of Kinetic Equations and Assignment of Simulation Rate Constants. The calculation of substrate hydrolysis rates from AChE reaction pathways in which reversible reactions are not at equilibrium is difficult because solutions to the corresponding differential equations are too complex for useful comparison to experimental data. We previously described our application of the program denoted SCoP (version 3.51), developed through the NIH National Center for Research Resources and available from Simulation Resources, Inc. (Redlands, CA), to solve these equations numerically (*18*). To obtain the simulated solutions to reaction schemes with the SCoP program, values for all reaction rate constants must be assigned or fitted. For Scheme 1, the second-order rate constant for substrate hydrolysis in the absence of inhibitor is given by eq 8.

$$\frac{k_{cat}}{K_{app}} = \frac{k_S k_2}{k_{-S} + k_2} \quad (8)$$

We previously showed (*18*) that values of k_S and k_{-S} in eq 8 could be assigned if (1) estimates of k_{cat}, K_{app}, and k_2 were

Table 1: Rate Constants for Simulated Substrate Hydrolysis and Substrate Inhibition with AChE[a]

substrate	k_S (μM^{-1} s^{-1})	k_{-S} (s^{-1})	k_1[b] (s^{-1})	k_{-1}[b] (s^{-1})	k_2, k_3 (s^{-1})	k_{-P}[c] (s^{-1})	k_{-P2}/k_{-P} (s^{-1})	*a*−*f*, *i*
acetylthiocholine	150[d]	2×10^5	3×10^6	4×10^4	1.4×10^4	1.3×10^5	0.01	1
M7A	200	4×10^4	8×10^4	4×10^3	1.4×10^4	1.3×10^3	0.01	1

[a] Simulations for both substrates were generated as outlined in the text with the indicated values of rate constants defined in Scheme 5 in the Appendix. [b] Calculated from eq 9 or 10 with an R_S that was assumed to be 1.0 (see Experimental Procedures). [c] Assigned from measured values for K_P of 0.66 ± 0.03 mM for thiocholine or 6.4 ± 0.6 μM for M7H as outlined in Experimental Procedures. [d] The extent of substrate inhibition with acetylthiocholine was measured at a constant ionic strength slightly higher than that in other experiments (see Experimental Procedures). Ionic strength affects primarily K_{app} but not k_{cat} (*12*); k_S, assumed to be the only rate constant sensitive to ionic strength, was recalculated from K_{app}.

available and (2) the solvent deuterium oxide isotope effects R, R_S, and R_2 were known, where R, R_S, and R_2 are the respective ratios of k_{cat}/K_{app}, k_S, and k_2 in H_2O to that in D_2O. When R_2 was assigned a typical value of 2.5 and R_S was assumed to be 1.0, for example, $k_S = 1.5(k_{cat}/K_{app})/(2.5 - R)$.

The second-order substrate hydrolysis rate constant in Scheme 3 in the Results is given by eq 9.

$$\frac{k_{cat}}{K_{app}} = \frac{k_S k_1 k_2}{k_{-S} k_{-1} + k_2 (k_{-S} + k_1)} \quad (9)$$

Assuming again that k_2 and k_S are the only intrinsic rate constants in this equation that are altered when H_2O is replaced by D_2O and that $R_2 = 2.5$, eq 10 may be derived.

$$\frac{k_S}{1 + \frac{k_{-S}}{k_1}} = \frac{1.5 k_{cat}}{K_{app}\left(2.5 - \frac{R}{R_S}\right)} \quad (10)$$

To assign the intrinsic rate constants in eq 9, we inserted independent estimates of k_{cat} and K_{app} into eq 10. For example, for acetylthiocholine and human AChE, we previously estimated that $k_{cat} = 7000$ s^{-1} and $k_2 = k_3 = 1.4 \times 10^4$ s^{-1} (*18*). With a measured value for K_{app} of 58 μM (Table 2 below), eq 10 requires that $k_S > k_{cat}/K_{app} = 120$ μM^{-1} s^{-1}. For M7A, we obtained k_{cat}/K_{app} from parallel measurements of V_{max}/K_{app} (as the constant $z_{I=0}$ in eq 2) for M7A and acetylthiocholine. The k_{cat}/K_{app} for M7A was 82 ± 2% of the k_{cat}/K_{app} for acetylthiocholine (data not shown). From our measured values of K_S [1.5 mM for acetylthiocholine (Figure 2B below) and 0.18 ± 0.01 mM for M7A (data not shown)], k_{-S} values were calculated from $k_{-S} = K_S k_S$. Assignments of k_1 and k_{-1} become problematic when R approaches 1.0 because of uncertainty in R_S. R_S has been considered to be as high as 1.25, the ratio of the viscosities of D_2O to H_2O at 25 °C (see, e.g., refs *30* and *31*). For acetylthiocholine, R = 1.21 ± 0.02 (*22*), and for M7A, $R = 1.09 \pm 0.05$ (data not shown); k_1 calculated from eq 10 was very sensitive to the values of both k_S and R_S. In practical terms, the simulations were not sensitive to the absolute values of k_S, k_1, and k_{-1} as long as k_1 was calculated from eq 10 and k_{-1} from eq 9. For example, simulated substrate inhibition curves for acetylthiocholine (Figure 3A below) were fitted to the Haldane equation (eq 1) by varying k_S from 120 to 500 μM^{-1} s^{-1} and calculating the corresponding values of k_{-S}, k_1, and k_{-1} (with all other rate constants fixed). The resulting fitted K_{app} and K_{SS} values varied by less than 5% (data not shown). We assigned k_S values of 200 μM^{-1} s^{-1} (at the ionic strength of buffer alone) to correspond to the general ligand association rate constant used in our previous simulations (*18*). The assigned values of k_2 and k_3 for M7A were the same as those for acetylthiocholine because (1) the k_3 reaction is identical with both substrates and (2) the simulations were quite insensitive to k_2 when k_2 exceeded k_{-P}; 8-fold increases or decreases in k_2 resulted in less than a factor of 2 change in fitted parameters when simulated v versus [S] curves were analyzed with the Haldane equation.

For all substrates, we obtained estimates of k_{-P} (Schemes 2 and 3) from $k_{-P} = K_I k_P$, where $K_I = K_P$ was the competitive inhibition constant for reaction product P measured with a different substrate. Since estimates of k_P are unavailable for any of the substrates used in this study, k_P was assumed to have the same value as k_S. The steric blockade parameter k_{-P2}/k_{-P} was assumed to be 0.01−0.04, consistent with our previous observations that ligand binding to the peripheral site decreases ligand dissociation rate constants from the acylation site by 10−100-fold (*18*). Assigned intrinsic rate constants for acetylthiocholine and M7A are summarized in Table 1.

RESULTS

Expansion of Our Steric Blockade Model To Include Inhibition of Product Dissociation. When a ligand binds to the peripheral site of AChE, the ensuing inhibition of substrate hydrolysis is often interpreted according to Scheme 1.

Scheme 1

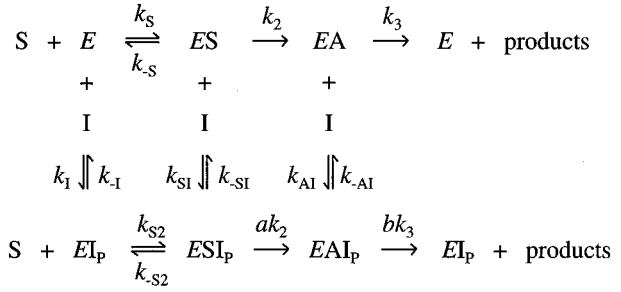

Inhibitor (I) can bind to each of the three enzyme species *E*, *E*S, and *E*A. For example, *E*SI$_P$ represents a ternary complex with substrate (S) at the acylation site and I at the peripheral site (denoted by the subscript P). The acylation rate constant k_2 is altered by a factor a in this ternary complex, and the deacylation rate constant k_3 is altered by a factor b in the *E*AI$_P$ complex. To obtain a tractable solution to the steady state substrate hydrolysis rate v that corresponds to Scheme 1, it has often been assumed that the reversible reactions are at equilibrium (with $k_{-X}/k_X = K_X$). Although this assumption cannot be justified for AChE (*1*), the mixed, partial inhibition patterns that are often observed with peripheral site inhibitors of AChE can be fitted to the equilibrium solution (*18*). These fits require that a (or b and

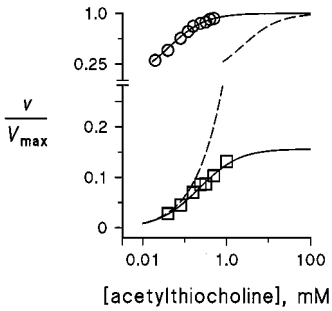

FIGURE 1: Propidium inhibition of the AChE-catalyzed hydrolysis of acetylthiocholine. Points represent initial velocities measured as outlined in Experimental Procedures at 25 pM AChE and the indicated acetylthiocholine concentrations with (□) or without (○) 50 μM propidium. Lines were generated by the SCoP simulation program for rate constants in Scheme 1 (O—O and - - -) or Scheme 4 (□—□). Rate constant values assigned previously (*18*) were as follows: $k_S = k_I = k_{SI} = k_{AI} = 200\ \mu M^{-1}\ s^{-1}$; $k_{S2} = 3\ \mu M^{-1}\ s^{-1}$; $k_{-S} = 3 \times 10^3\ s^{-1}$; $k_{-S2} = 45\ s^{-1}$; $k_{-I} = k_{-SI} = k_{-AI} = 200\ s^{-1}$; $k_2 = k_3 = 1.4 \times 10^4\ s^{-1}$; and $a = b = 1$. New rate constants required to extend Scheme 1 to Scheme 4 were assigned as follows: $k_{-P} = 6 \times 10^4\ s^{-1}$; $k_{-P2} = 9 \times 10^2\ s^{-1}$; and $c = d = e = f = i = 1$.

K_S/K_{S2}) be much less than 1, and interpretation of such low values would appear to indicate a conformational interaction between the two sites.

To avoid assumptions of equilibrium in Scheme 1, we introduced a nonequilibrium analysis that involved numerical solution of the rate equations that arise from Scheme 1 with the SCoP program (*18*). The analysis required assignment of all the rate constants in Scheme 1 and generated simulated values of v. We simplified these assignments by proposing our steric blockade model in which the only effect of bound peripheral site ligand is to decrease k_{S2} relative to k_S and k_{-S2} relative to k_{-S} while maintaining $K_S = K_{S2}$ and $a = b = 1$. Since k_S is rate-limiting at low substrate concentrations without inhibitor and k_{S2} becomes rate-limiting at low substrate concentrations and saturating concentrations of inhibitor, the model with Scheme 1 correctly predicts that increasing concentrations of inhibitor should progressively decrease the second-order hydrolysis rate measured at low substrate concentrations (*18*). However, at high substrate concentrations, neither k_S nor k_{S2} remains rate-limiting, and the model with Scheme 1 predicts that inhibitor should have no effect on the V_{max} obtained at high substrate concentrations. This prediction is not supported experimentally, as illustrated in Figure 1. This figure shows v as a function of acetylthiocholine concentration. In the absence of propidium, the observed v (○) were fitted well by the line simulated with the steric blockade model. With the peripheral site occupied by a saturating concentration of propidium (50 μM), the simulated v (dashed line) corresponded well with the observed v (□) at low substrate concentrations but increased much more than the observed v at higher substrate concentrations. Near 100 mM acetylthiocholine, the simulated lines for v with and without propidium converged. Therefore, the steric blockade model with Scheme 1 fails to incorporate an inhibition component that becomes apparent at high substrate concentrations. This inhibition component might involve substrate inhibition, a phenomenon observed with some cationic substrates such as acetylthiocholine that is addressed below. However, the experimental acetylthiocholine concentrations in Figure 1 are below the range where substrate inhibition is observed. Furthermore, the divergence in Figure 1 between simulated and observed v values in the presence of propidium is also seen with other substrates such as phenyl acetate that do not exhibit substrate inhibition (*18*).

Schemes 2 and 4 incorporate a logical extension of Scheme 1 which, as we now show, can eliminate disagreement between the steric blockade model and observed v at the higher substrate concentrations investigated experimentally in Figure 1. Scheme 2 makes explicit the dissociation rate constant k_{-P} for the first product P, the alcohol leaving group (e.g., thiocholine) generated by acylation of the active site serine. For simplicity, inclusion of a peripheral site inhibitor is deferred to Scheme 4 in the Appendix.

Scheme 2

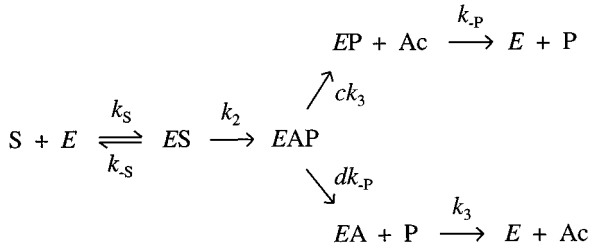

The first intermediate following enzyme acylation in Scheme 2 is *E*AP. To maintain generality, P may dissociate before (dk_{-P}) or after (k_{-P}) the deacylation step. *E*AP has not been included explicitly in most catalytic pathways previously considered for AChE because dk_{-P} has been assumed to be sufficiently fast to render any accumulation of *E*AP negligible. This appears to be a good assumption for most AChE substrates. For example, we estimated k_{-P} for acetylthiocholine to be $1.3 \times 10^5\ s^{-1}$ from the relationship $k_{-P} = k_P K_P$, where a K_P of 0.66 mM was measured as the competitive inhibition constant for thiocholine inhibition of M7A hydrolysis (data not shown) and the association rate constant k_P for thiocholine was assigned the same value assumed for acetylthiocholine ($200\ \mu M^{-1}\ s^{-1}$). Since this k_{-P} is nearly 1 order of magnitude larger than k_2 or k_3, its inclusion in the model has little effect on the experimental kinetic parameters; calculations based on Schemes 1 and 2 (with $d = 1$) show that k_{cat} is decreased by less than 1% and k_{cat}/K_{app} is unaltered.

We extend our steric blockade hypothesis with Scheme 4 (Appendix) by proposing that a bound peripheral site inhibitor not only reduces association and dissociation rate constants for substrate binding to the acylation site but also reduces the dissociation rate constant for release of P. In this case, a simulated nonequilibrium analysis demonstrates that product dissociation rate constants can become important. A key rate constant in this analysis was k_{-P2}, the rate constant for dissociation of P from the EPI_P ternary complex, since our steric blockade model proposes that the only consequences of ligand binding to the peripheral site are low ratios of k_{S2}/k_S, k_{-S2}/k_{-S}, and k_{-P2}/k_{-P}. For example, if bound propidium at the peripheral site reduced k_{-P2} in Scheme 4 to 1.5% of k_{-P}, the same reduction previously deduced for k_{-S2} relative to k_{-S} for acetylthiocholine (*18*), then thiocholine dissociation does contribute to a reduction in v. With a k_{-P} of $1.3 \times 10^5\ s^{-1}$ as calculated above, most of the divergence between the experimental points with 50 μM propidium and the corresponding simulated line in Figure 1 was eliminated. Assigning just a 2-fold lower value of k_{-P} ($6 \times 10^4\ s^{-1}$) completely eliminated this divergence and gave the simulated

lower line shown in Figure 1. Therefore, if product affinity for the acylation site is sufficiently high, product release may become partially rate-limiting when the peripheral site is occupied. Specifically, v will be affected when the product dissociation rate constant k_{-P2} falls within the range of the acylation (k_2) and deacylation (k_3) rate constants. Thiocholine, a cationic leaving group P, illustrates this point in Figure 1. In contrast, the acetate product (Ac) of acetylthiocholine hydrolysis has an affinity for the acylation site that is too low (K_I > 100 mM) to contribute any rate limitation even with propidium bound to the peripheral site. The analysis in Figure 1 completes our demonstration that the steric blockade can explain AChE inhibition by peripheral site ligands. Specifically, direct measurement of association and dissociation rate constants for the acylation site ligands huperzine A and TMTFA revealed decreases of 10−380-fold when propidium was bound to the peripheral site (*18*), and decreases in these rate constants alone for substrates and their hydrolysis products are sufficient to account for inhibition by bound peripheral site ligands at both low (*18*) and high (Figure 1) substrate concentrations.

Acetylcholine Can Bind to the Peripheral Site. We turn next to the questions of whether acetylthiocholine, a close analogue of the physiological substrate acetylcholine, can bind to the peripheral site and whether this binding is of significance on the catalytic pathway. Scheme 3 defines an initial complex ES_P of substrate with the peripheral site and incorporates this species into the previous catalytic pathway from Scheme 2.

Scheme 3

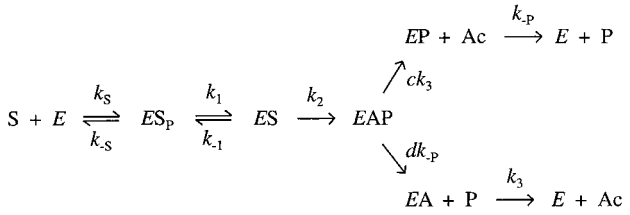

ES_P can reversibly proceed to ES, the complex of substrate with the acylation site, where acylation occurs. For simplicity, we have not included the additional complexes ESS_P, $EAPS_P$, EAS_P, and EPS_P in Scheme 3, but they are made explicit in Scheme 5 in the Appendix. These complexes are important in the phenomenon of substrate inhibition considered below, and they also must be considered in any measurement of substrate affinity for the peripheral site.

A direct way of measuring substrate affinity for the peripheral site is to measure the effect of substrate on the association rate constant k_{on} for a slowly equilibrating ligand that binds exclusively to the peripheral site. Fasciculin is such a ligand, and we previously confirmed the affinity of propidium for the peripheral site by measuring its inhibition constant K_I during fasciculin binding (*22*). The analysis was straightforward with an inhibitor like propidium (I) that competes with fasciculin, because only a single complex EI_P is formed to alter the observed k_{on}. If our steric blockade model is correct and ligand binding to the peripheral site is unaffected by the presence of ligands or an acyl group at the acylation site, then this analysis can be extended directly to include substrate. Only species with S bound to the peripheral site are relevant, and the resulting analysis should

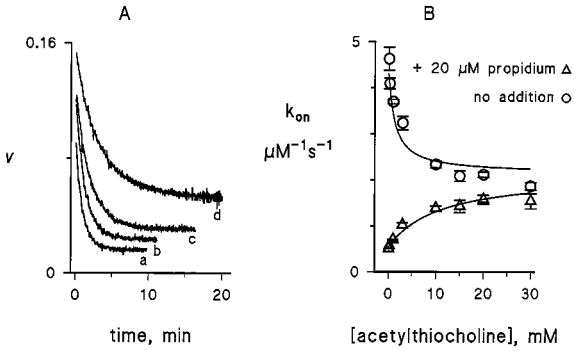

FIGURE 2: Acetylthiocholine binding to the AChE peripheral site. (A) The hydrolysis rate v (ΔA_{412nm} per minute) for the approach to equilibrium fasciculin (F) binding was measured with 10 mM acetylthiocholine, 50 pM AChE, F (a, 5 nM; b, 3 nM; c, 2 nM; and d, 1 nM), and buffered 50 mM NaCl by continuous spectrophotometric assay as outlined in Experimental Procedures. Rate constants (k) obtained from eq 4 were then plotted against the fasciculin concentration (eq 5) to obtain k_{on} (plot not shown). (B) The dependence of k_{on} on the acetylthiocholine concentration was analyzed with eqs 6 and 7. Indicated points representing the average of three or four k_{on} measurements (except at 15 mM) were fitted with eq 6 to give apparent K_S estimates of 3.6 ± 1.0 mM in the absence of propidium (○) and 0.6 ± 0.1 mM with 20 μM propidium (△). (This fitting is not shown here but is given in Figure 2B of ref *45*.) A mean K_S of 1.5 mM was used to assign k_{-S} in Table 1 and to generate *both* lines representing the simulated dependence of k_{on} on [S] from eq 7. The simulations were based on Scheme 5 as outlined in the text with the rate constant assignments in Table 1 except that $k_{-P} = 6 \times 10^4$ s^{-1}; in addition, k_{-I} and k_{-P2} for propidium were the same as in Figure 1 but $k_I = 70$ μM^{-1} s^{-1} (due to the change in ionic strength from Figure 1). The simulated lines also were fitted well by eq 6 with a K_S value of 1.36 ± 0.01 mM both in the absence of propidium and with 20 μM propidium.

be compatible with eq 6. However, in the presence of both S and I, Scheme 5 includes 14 liganded enzyme species as noted in the Appendix. It is certainly possible that our model is oversimplified and that ligands bound to the acylation site will alter ligand binding to the peripheral site. We can address this possibility by simulation analysis of the more general eq 7. We began our experimental analysis by measuring the observed rate constants k for fasciculin binding during continuous substrate hydrolysis as shown in Figure 2A. Apparent association rate constants k_{on} were then calculated from a series of k values obtained at fixed acetylthiocholine concentrations [S] according to eq 5. Plots of k_{on} versus [S] in the absence of propidium revealed that k_{on} did decrease at higher S concentrations and reasonably conformed to eq 6 (○ in Figure 2B). This decrease suggested that acetylthiocholine competes with fasciculin at the peripheral site, but to our surprise, the competition was only partial. Values of k_{on} at high S concentrations leveled off at about one-half of the k_{on} extrapolated to zero S concentration. According to eq 6, this observation indicates that k_{FP} for fasciculin binding to ES_P is about one-half of k_F, the intrinsic association rate constant for fasciculin binding to the peripheral site in free AChE. In contrast, k_{on} for fasciculin was observed previously to decrease to near zero at high propidium concentrations, and the absence of any detectable k_{FP} for fasciculin with the propidium−AChE complex was taken as evidence that fasciculin and propidium were completely competitive (*22*). Our immediate concern was that the partial acetylthiocholine inhibition of fasciculin binding did not reflect an interaction

of acetylthiocholine at the peripheral site but instead was an indirect effect of acetylthiocholine bound at the acylation site. Three points argued against this interpretation. First, the apparent K_S for the acetylthiocholine that competes with fasciculin according to eq 6 was in the low millimolar range (Figure 2B). This value was nearly 2 orders of magnitude higher than K_{app} for acetylthiocholine, which roughly indicates the affinity of substrate complexes at the acylation site. Second, inclusion of edrophonium, an inhibitor specific for the acylation site, at high concentrations (90 times its K_I) with acetylthiocholine and fasciculin only slightly altered the upper plot in Figure 2B (data not shown). Third, when in contrast a high concentration of propidium (nearly 10 times its K_I) was included, progressively higher S concentrations actually increased the observed k_{on} substantially (△ in Figure 2B). Since propidium affinity for the peripheral site is at most slightly affected by the binding of ligands to the acylation site (*9*, *18*), this observation appears to require that acetylthiocholine and propidium compete at the peripheral site and that displacement of propidium by acetylthiocholine result in an increased rate of fasciculin association.

To confirm this indication of acetylthiocholine binding to the peripheral site, we conducted nonequilibrium simulations in which k_{on} was calculated from eq 7. Differential equations corresponding to the rate expressions from Scheme 5 were solved numerically by the SCoP program with rate constants (Table 1 and Figure 2B) assigned as outlined in Experimental Procedures. The geometric mean of the apparent K_S estimates from eq 6 with and without propidium was about 1.5 mM (Figure 2B), and from this value and the previously estimated k_S, a k_{-S} of 2×10^5 s^{-1} was assigned. Two other key assignments involved the relative values of k_{FP}/k_F and k_{FA}/k_F in eq 7. The decision to limit the 14 possible fasciculin association rate constants to only these three in the numerator in eq 7 was largely based on the close conformity of the data in Figure 2B to eq 6. This conformity indicated that fasciculin associated with several enzyme species with identical rate constants. We sorted these enzyme species into four groups. The first consisted of those with no bound cationic ligands (i.e., $[E] + [EA]$) with a fasciculin association rate constant of k_F. The second contained those in which substrate was bound to the peripheral site ($\sum ES_P$) and was characterized by a relative rate constant of k_{FP}/k_F. The third included those in which the peripheral site was free but substrate or its thiocholine product was bound to the acylation site ($\sum EX_A$), and these were given a relative rate constant of k_{FA}/k_F. The fourth involved those with propidium bound to the peripheral site ($\sum EI_P$) and with a relative rate constant of zero. We first simulated our steric blockade model, in which ligand binding to the peripheral site is unaffected by the presence of ligands or an acyl group at the acylation site. Fasciculin association was assumed to be partially blocked by substrate bound at the peripheral site ($k_{FP}/k_F = 0.5$) but unaffected by substrate or product bound at the acylation site ($k_{FA}/k_F = 1$). In support of the latter assignment, previous data (*22*) and our results above indicated that fasciculin association rate constants are not affected by edrophonium bound to the acylation site. With these assignments, the simulation program calculated the concentrations of all the enzyme intermediates in Scheme 5, with and without propidium, and solved eq 7 for k_{on} as a function of S concentration. The simulated values of k_{on} are shown as the lines in Figure 2B. They superimposed well with the original fits of the experimental data to eq 6, and they confirmed that eq 6 provides an excellent approximation when fasciculin association is affected only by substrate bound to the peripheral site. The K_S of 1.4 mM calculated from the simulations agreed with the assigned K_S. In contrast, when both k_{FP}/k_F and k_{FA}/k_F were assigned a value of 0.5, the simulated K_S with 20 μM propidium was unchanged but the simulated K_S without propidium decreased 5-fold. This trend was the opposite of that observed experimentally in Figure 2B. We also examined whether a small decrease in the relative fasciculin association rate with substrate or product bound to the acylation site ($k_{FA}/k_F = 0.5$) could be superimposed on complete competition between substrate and fasciculin at the peripheral site ($k_{FP}/k_F = 0$). In this case, the simulations showed that k_{on} with 20 μM propidium did not change significantly with increased S concentrations, again in contrast to the observations in Figure 2B. These simulations confirmed the indication in the previous paragraph that acetylthiocholine and propidium must compete at the peripheral site for acetylthiocholine to accelerate fasciculin association in the presence of propidium.

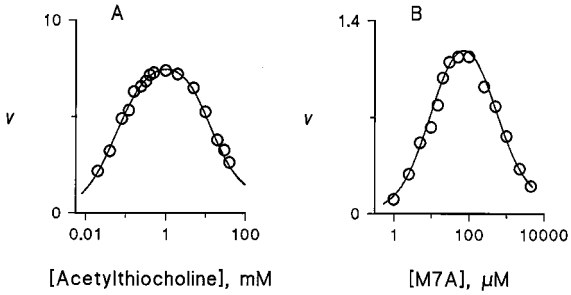

FIGURE 3: Substrate inhibition with acetylthiocholine and M7A. Points represent initial velocities (μM min^{-1}) measured at the indicated substrate concentrations as outlined in Experimental Procedures. (A) Reaction mixtures with acetylthiocholine and 20 pM AChE were supplemented with NaCl such that [S] + [NaCl] = 60 mM to maintain a constant ionic strength. The line was generated by the SCoP simulation program with assigned rate constants in Table 1 except that $k_{-P} = 6 \times 10^4$ s^{-1}. When fitted to the Haldane equation (eq 1), the simulated line corresponded to a K_{app} of 57.9 ± 0.4 μM and a K_{SS} of 17.9 ± 0.1 mM. (B) Initial velocities for M7A in 20 mM sodium phosphate buffer with the experimental AChE concentrations (20−2000 pM) were normalized to 20 pM AChE for comparison to Figure 3A. The line was generated by the SCoP simulation program with assigned rate constants in Table 1 except that k_{-P} was slightly increased to 1.5×10^3 s^{-1} and thermodynamic interaction between sites was allowed, with $i = 4$, $k_{-S} = 2 \times 10^4$ s^{-1}, $k_1 = 4 \times 10^4$ s^{-1}, and $k_{-P2}/k_{-P} = 0.04$. When fitted to the Haldane equation, the simulated line corresponded to a K_{app} of 9.3 ± 0.1 μM and a K_{SS} of 640 ± 3 μM.

Since the individual rate constants on the catalytic pathway in Scheme 3 in general are too high to measure by rapid kinetic techniques, there are relatively few phenomena involving substrate hydrolysis by AChE that allow us to obtain experimental evidence to support Schemes 3 and 5 and the rate constant assignments in Figure 2B. Two pertinent phenomena are substrate inhibition and mixed substrate hydrolysis, and these are examined in the following sections.

Substrate Inhibition. When rates of acetylthiocholine hydrolysis with AChE are measured as a function of acetylthiocholine concentration [S], the profile in Figure 3A is observed. This profile does not correspond to a simple

Table 2: Simulated and Observed Kinetic Parameters for Substrate Hydrolysis and Substrate Inhibition with AChE[a]

substrate	k_{cat} (s^{-1})	K_{app} (μM)	K_{SS} (mM)
	Observed Values		
acetylthiocholine	7000[b]	58 ± 2	18.6 ± 0.7
M7A	1300 ± 160[c]	10 ± 1	0.7 ± 0.1
	Simulated Values		
acetylthiocholine	*d*	*d*	44.4 ± 0.1
M7A	1120 ± 30[c]	8.8 ± 0.04	0.25 ± 0.001

[a] Kinetic parameters were determined by fitting the dependence of v on the substrate concentration to the Haldane equation (eq 1). Simulated values were obtained with Scheme 5 (Appendix) and the rate constants in Table 1. [b] From previous literature values (see ref *18*). [c] Calculated from the product of $k_{cat}/K_{app} \times K_{app}$. [d] Matched to observed parameters by rate constant assignments.

Michealis−Menten kinetic pattern, and the bell-shaped curve with the decline at high S concentrations has long been referred to as substrate inhibition (*32*). This curve can be fitted to the Haldane equation (eq 1), which contains three experimental parameters: V_{max} ($= k_{cat}[E]_{tot}$), K_{app}, and the substrate inhibition constant K_{SS}. Since the Haldane equation is not restricted to any mechanistic scheme, it provides a useful quantitative standard for assessing data simulated from our nonequilibrium analysis of Scheme 5 with the rate constant assignments in Table 1. It is important to note that these rate constants were assigned from data unrelated to the substrate inhibition phenomenon itself.

For acetylthiocholine K_{SS} was the only parameter independently obtained from this fitting procedure, as known values of k_{cat} and K_{app} were incorporated into the rate constant assignments. The simulation in fact generated a curve exhibiting substrate inhibition with a K_{SS} value of 44.4 mM, about twice the observed K_{SS} of 18.6 mM (Table 2). We assessed changes in assigned rate constants that could reconcile this difference. Although substrate inhibition results from a low value of k_{-P2}/k_{-P}, the value of K_{SS} obtained from the simulation was only moderately sensitive to the k_{-P2}/k_{-P} assignment (e.g., changing k_{-P2}/k_{-P} from 0.01 to 0 only decreased the simulated K_{SS} to 28 mM). In contrast, the simulated K_{SS} value was more sensitive to the assigned value of k_{-P}, with the two values appearing virtually proportional. For example, decreasing the assigned k_{-P} from 1.3×10^5 to 6×10^4 s^{-1} decreased the K_{SS} obtained from the simulation to 17.9 mM and gave an excellent fit of the simulated curve to the experimental data, as shown in Figure 3A. Since the original assignment of k_{-P} assumed that $k_P = k_S$, an assumption that cannot be tested experimentally with available techniques, the agreement between the observed and simulated substrate inhibition data appears to be quite reasonable.

We next turned to M7A, a substrate that previously exhibited substrate inhibition with eel AChE (*26*, *33*) and also showed this inhibition pattern with human AChE (Figure 3B). This substrate is of particular interest in testing our steric blockade model because it binds to the peripheral site ($K_S = 0.18 \pm 0.01$ mM from competition with fasciculin, data not shown), and its hydrolysis product M7H has a high affinity for AChE and a consequent low calculated k_{-P} of 1.3×10^3 s^{-1} (Table 1). Analysis of the simulated v versus [S] curve with the Haldane equation and the constants for M7A in Table 1 gave independent estimates of K_{SS} and k_{cat}, since only the ratio k_{cat}/K_{app} was incorporated into the rate constant assignments. The simulated K_{SS} of 0.25 mM was nearly 3 times smaller than the observed K_{SS} of 0.7 mM, but the simulated k_{cat} was within 20% of that observed (Table 2). The reasonably close agreement supported our steric blockade model. In particular, the observed k_{cat} for M7A was only 19% of the k_{cat} for acetylthiocholine (Table 2), and this low relative k_{cat} was explained in the steric blockade model by the low k_{-P} for the M7H product. In contrast to the interaction of acetylthiocholine with AChE, the most abundant simulated intermediate with M7A at concentrations below K_{SS} was *E*P, the AChE complex with the M7H product, and dissociation of this complex was the step that limited the value of k_{cat}. As a consequence, a slight increase in k_{-P} resulted in an almost proportionate increase in k_{cat} but in almost no effect on K_{SS}. The most straightforward way to achieve agreement between the simulated and observed K_{SS} values[2] was to relax the stringent assumption in our steric blockade model that the affinity of ligands for the peripheral and acylation sites was unchanged when both sites were occupied simultaneously in a ternary complex (see Discussion). Good agreement was then observed in Figure 3B, where the affinities of M7A and M7H in ternary complexes were assigned to be 25% of their affinities in binary complexes (e.g., $i = 4$). The simulation in Figure 3B also assumed that the apparent K_S of 0.18 mM for M7A was an average of the actual K_S and of iK_S, where iK_S is the dissociation constant for M7A binding to the peripheral site when the acylation site is occupied by M7A or M7H.

Mixed Substrate Hydrolysis. When two substrates are mixed with AChE, each substrate inhibits the hydrolysis of the other. We measured the extent of competitive inhibition of acetylthiocholine hydrolysis by M7A and, conversely, the extent of competitive inhibition of M7A hydrolysis by acetylthiocholine by monitoring the hydrolysis of each substrate independently. Competitive inhibition was assessed from relative second-order hydrolysis rate constants z by plotting the data according to eq 3. If none of the enzyme intermediates generated by the competing substrate can react with the monitored substrate, then the K_I for the competing substrate should equal its K_{app}. This is typically the case for simple models of substrate competition, and it is also the case when M7A is the competing substrate during acetylthiocholine hydrolysis. In Figure 4A, the solid line represents the inhibition calculated from eq 3 when K_I for M7A equals its K_{app} from Figure 3B. The observed points were within experimental error of this line. Furthermore, simulation of this competition with the steric blockade model applied to Scheme 5 and the assigned rate constants in panels A and B of Figure 3 generated the dashed line that also closely followed the solid line. The data indicate that acetylthiocholine does not initiate its catalytic pathway with any

[2] Assigned rate constants could also be adjusted in the following way to obtain agreement of the simulated and observed K_{SS} for M7A in Figure 3B. A 7-fold decrease in k_2 combined with a 3-fold increase in k_{-P}, relative to the assignments in Table 1, shifted the rate-limiting step in k_{cat} from product dissociation to acetylation and gave a simulated curve virtually identical to the one in Figure 3B. These adjustments were not a very attractive option because they seem to run counter to observations that the M7H leaving group promotes excellent acylation of AChE. For example, dimethylcarbamoylated M7H shows a higher acylation rate constant than dimethylcarbamoylated choline (*25*, *34*). Furthermore, these adjustments gave a less than satisfactory fit of the simulated curve to the experimental points in Figure 4B.

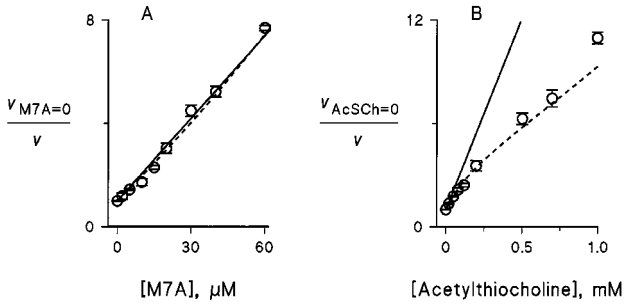

FIGURE 4: Inhibition of hydrolysis of one substrate by a second substrate. (A) Points denote second-order rate constants z for acetylthiocholine (AcSCh) measured in the presence of competing M7A as the inhibitor (see Experimental Procedures). The points were normalized to $z_{M7A=0}$ for acetylthiocholine in the absence of M7A and plotted according to eq 3. (B) Points denote second-order rate constants z for M7A in the presence of competing acetylthiocholine (AcSCh) normalized to $z_{AcSCh=0}$ for M7A in the absence of acetylthiocholine. M7A hydrolysis was monitored by spectrofluorometry. In each panel, indicated points represent averages of two to four measurements. The solid line is the extent of calculated inhibition if the K_I for the competing substrate were equal to its K_{app}. The dashed line is the extent of inhibition simulated for the steric blockade model with Scheme 5 and the assigned rate constants in panels A and B of Figure 3. New rate constants resulting from mixed ternary complexes (e.g., $i_{ST} = i_{TS} = 1$, see Appendix) were assigned assuming no thermodynamic interaction between the bound ligands in these complexes.

enzyme intermediate produced by M7A. However, when acetylthiocholine is the competing substrate during M7A hydrolysis, the observed inhibition points fell below the solid line expected if K_I for acetylthiocholine were equal to its K_{app} (Figure 4B). A similar pattern of inhibition of M7A hydrolysis by acetylthiocholine was observed previously with eel AChE (*26*). The level of inhibition in Figure 4B corresponded well to the level of inhibition simulated with Scheme 5 (dashed line in Figure 4B), thereby supporting our steric blockade model. The simulation was particularly sensitive to two parameters, k_{-S} for M7A and k_{-P2}/k_{-P} for thiocholine product dissociation when M7A was bound to the peripheral site. A decrease in k_{-S} or an increase in this k_{-P2}/k_{-P} resulted in less inhibition by acetylthiocholine. This pattern indicates that an M7A molecule can initiate its catalytic pathway by binding to the peripheral site when acetylthiocholine is bound to the acylation site. The dissociation of this M7A is sufficiently slow that it will *wait* at the peripheral site while acetylation by the acetylthiocholine and deacetylation occur and the thiocholine product dissociates from the enzyme. This M7A then will proceed to the acylation site. A corresponding phenomenon is not seen during M7A inhibition of acetylthiocholine hydrolysis because acetylthiocholine dissociates too rapidly from the peripheral site and product M7H dissociates too slowly from the acylation site. These data provide the most direct evidence in support of our proposal in Schemes 3 and 5 that initial substrate binding to the peripheral site occurs on the catalytic pathway. This pathway does not require release of substrate from the peripheral site to the solution and its direct reassociation with the acylation site for catalysis to occur.

DISCUSSION

A key observation in this report is that acetylthiocholine can bind to the AChE peripheral site with an equilibrium dissociation constant K_S of about 1 mM. This value was determined from the effect of the acetylthiocholine concentration on the rate at which fasciculin associates with the peripheral site. The approach to equilibrium fasciculin binding was monitored by continuous spectrophotometric assay of acetylthiocholine hydrolysis. We employed this method previously with the high-affinity bisquaternary inhibitor ambenonium and found that acetylthiocholine inhibited ambenonium association by binding to a site on AChE with a K_S of about 1 mM (*29*), in good agreement with our current estimate. However, since ambenonium binds to both the acylation and peripheral sites simultaneously, it was difficult to assign this acetylthiocholine binding to the peripheral site. Our current assay has the advantages that fasciculin binds only to the peripheral site and that its slower rate of binding allows greater precision. Noise levels with the Cary 3A spectrophotometer are low enough to allow velocity estimates over 2 s intervals, and rate constants (k) for the approach to equilibrium fasciculin binding (Figure 3A) were fitted with typical standard errors of 1−5%.

When acetylthiocholine binding to the peripheral site is incorporated into our steric blockade model, a wide range of kinetic data, including substrate inhibition, can be explained. To keep the model conceptually simple, we have examined the very limited hypothesis that the only effect of substrates or inhibitors bound to the peripheral site is to decrease association and dissociation rate constants for acylation site ligands without changing their ratio, the equilibrium dissociation constant. Thus, we hypothesize that a bound peripheral site ligand has no effect on the thermodynamics of binding of acylation site ligands or on their reactivity at the acylation site. Even with this assumption, some of the rate constants in Schemes 3 and 5 cannot be assigned uniquely. The simulations revealed that an important assignment is the rate constant for product dissociation k_{-P}. This rate constant has not been measured directly for either thiocholine or M7H, the hydrolysis products of the substrates examined here. It is therefore reassuring that a single assignment for k_{-P} of 6×10^4 s^{-1} for thiocholine results in excellent agreement of the simulations with the observed data for propidium inhibition of acetylthiocholine hydrolysis (Figure 1), acetylthiocholine competition with fasciculin and propidium (Figure 2B), and substrate inhibition with acetylthiocholine (Figure 3A). While we are convinced that the steric blockade model offers the best understanding to date of ligand interactions with AChE, further refinements can be made. For example, we noted previously that association rate constants were decreased more than dissociation rate constants for both huperzine A and TMTFA when propidium was bound to the peripheral site (*18*). The difference corresponded to about a 5-fold decrease in affinity for the ligands in the ternary complex relative to the affinities of either ligand in the binary complexes with the free enzyme. We suggested that this difference might reflect an electrostatic interaction between these cationic ligands in the ternary complexes, and we do not view it as a serious challenge to the general steric blockade model. In terms of Scheme 4 or 5, this refinement would dictate a larger value of k_{-S2}/k_{-S} than of k_{S2}/k_S and in turn require thermodynamically that i be greater than 1. Increasing i to 4 gave the best agreement of the simulated and the observed data for M7A in Figures 3B and 4. Furthermore, when similar changes were incorporated into the simulations for acetylthiocholine with eq 7

in Figure 2B and the simulated data were then fitted with eq 6, a higher K_S was obtained without propidium than with propidium. This appears to be an improvement, because a similar divergence in K_S values was seen in our experimental fits in Figure 2B. However, these simulations for acetylthiocholine also require small adjustments in other assigned rate constants, and we have not attempted to find a self-consistent set of adjustments that would retain the agreement of the simulations to the observed data for acetylthiocholine in Figures 1, 2B, 3A, and 4 noted above.

The steric blockade model in Schemes 3 and 5 resolves a long controversy over the mechanistic interpretation of substrate inhibition with AChE. The controversy involved two alternative mechanisms. One proposal was that substrate inhibition arises from S binding to the anionic site of acetylated AChE to give an *E*AS complex in which deacylation is blocked (*26*, *35*−*37*). This proposal predicted that the substrate inhibition constant K_{SS} fitted by the Haldane equation (eq 1) will depend not only on the substrate affinity in *E*AS but also on the relative amount of *E*A. It was supported by observations that uncompetitive inhibition constants as well as K_{SS} increased for substrates with a lower k_{cat} (since these formed less *E*A). Alternatively, it was proposed that substrate inhibition arises from binding of two molecules of S in an *E*SS complex in which enzyme acetylation is blocked. Either the two S molecules could bind in the acylation site (*38*), or one S could bind in the acylation site and one in the peripheral site (*39*, *40*). This proposal predicted that K_{SS} from the Haldane equation should equal the dissociation constant for the lower-affinity S site in the *E*SS complex. It was supported when values for K_S of 15−25 mM for acetylcholine or acetylthiocholine binding to the peripheral site, determined by competition in a fluorescence titration of propidium with DFP-inactivated AChE, were the same as the corresponding K_{SS} estimates (*40*). It is unclear why these K_S estimates are so much higher than those we have determined from acetylthiocholine inhibition of the association reactions of ambenonium (*29*) or fasciculin (Figure 2B) with the peripheral site.[3] Our steric blockade model combines features from both of these proposals and extends them in a nonequilibrium context. The complex responsible for inhibition is neither *E*AS nor *E*SS but instead is EPS_P. This intermediate accumulates because S binding to the peripheral site blocks the dissociation of P, a feature that agrees with the contention in the second proposal that substrate bound to the peripheral site is responsible for substrate inhibition. Furthermore, for a series of substrates with similar K_S and k_{-P} values but varying k_2 values, K_{SS} will increase as k_{cat} decreases. Thus, our steric blockade model can account for the variations in K_{SS} which originally led to the first proposal.

Some previous reports (*5*) have noted that measured v values at high S concentrations fall above the overall substrate inhibition curve fitted to the Haldane equation (eq 1). Such deviations have been attributed to a low acetylation activity in the ESS complex. While no significant deviations of this type were observed over the range of S concentrations investigated in our experiments, it is worth noting that such deviations can be accounted for within our steric blockade model. As k_{-P2}/k_{-P} increases from the low value of 0.01 assumed in Table 1, simulated values of v at high S concentrations fall above the curve predicted by the Haldane equation because the rate of product dissociation even with S bound to the peripheral site makes a significant contribution to v.

Our observation in Figure 2B that acetylthiocholine and fasciculin were only partially competitive in binding to the peripheral site was unexpected. From our analyses with eqs 6 and 7, k_{FP} for fasciculin binding to the ES_P complex was nearly 50% of the k_F for fasciculin binding to the free enzyme. However, these equations do not address the stability of the ES_PF_P complex in which both acetylthiocholine and fasciculin are bound to the peripheral site. To explore the stability of this complex, we considered an extension of Schemes 4 and 5 in which a set of 20 complete time courses for fasciculin binding in the presence of acetylthiocholine (e.g., like those in Figure 2A) were fitted with the SCoP program (see examples involving TMTFA binding in ref *18*). Only rough approximations were attempted because fasciculin exerts a conformational effect on the acylation site in addition to its steric blockade (i.e., $a < 1$; *18*, *22*). However, the fitting procedure indicated a 2−3 order of magnitude decrease in the affinities of acetylthiocholine and fasciculin in this ES_PF_P ternary complex relative to the affinities of either ligand in the binary complexes with the free enzyme. To rationalize the formation of this ternary complex, we reviewed the kinetic properties of previously reported AChE mutants and examined the crystal structures of the fasciculin−AChE complexes (*7*, *8*) to identify a potential acetylthiocholine binding site that largely overlaps with that of propidium but only slightly overlaps with that of fasciculin. D72 is a residue midway along the active site gorge that some reports have included in the peripheral site, and its mutation decreases k_{cat}/K_m for acetylthiocholine about 50-fold (*5*). D72 appears to be important in the initial binding of TMTFA, because mutation to D72N reduced the overall TMTFA association rate constant at high ionic strengths more than 20-fold without an effect on the corresponding rate constant for the neutral analogue of TMTFA (*15*). D72 also was shown to be responsible for the enhanced reactivity of cationic organophosphates relative to their uncharged counterparts (*41*). Since D72 does not make contact with fasciculin in the crystal structures, it appears to be possible that acetylthiocholine could interact with D72 and still allow a nearly normal association rate constant for the binding of fasciculin to the remainder of the peripheral site to form the ternary complex. Studies with D72 mutants are currently underway to examine this possibility.

Our discussion of the steric blockade model has focused entirely on the point that ligand binding to the peripheral site can have an inhibitory effect on substrate turnover at the acylation site. However, inhibitor binding to the peripheral site is not apparent in vivo and thus is not suspected to play any regulatory role under physiological conditions of acetylcholine hydrolysis by AChE. Furthermore, the concentrations of acetylcholine itself are not high enough to give rise to any significant substrate inhibition during synaptic

[3] Preliminary measurement of K_S for *Torpedo* AChE gave a value of about 0.5 mM with techniques identical to those in Figure 2 (T. Szegletes, W. D. Mallender, and T. L. Rosenberry, manuscript in preparation), indicating that the higher affinity of acetylthiocholine for the peripheral site reported here is not unique to human AChE. We suspect that the lower affinities in the previous reports were subject to technical limitations.

transmission at the neuromuscular junction (*42*). Therefore, it is important to note that our model indicates a key role for the peripheral site under physiological conditions in which AChE is not saturated with acetylcholine. The hydrolysis rate v under these conditions is proportional to the second-order rate constant k_{cat}/K_{app} as given by eq 9, and initial binding of the substrate to the peripheral site increases this rate constant in several ways. It increases k_S because the peripheral site enlarges the enzyme surface and increases the frequency of productive substrate encounters; it decreases k_{-S} and thus allows a greater proportion of substrate molecules initially associated with the peripheral site to proceed to the acylation site, and it may well accelerate k_1 by optimally positioning substrate to diffuse rapidly into the acylation site.

Most previous kinetic analyses of AChE have employed equilibrium interpretations of reaction schemes similar to that in Scheme 1. Under what conditions do the conclusions from these analyses remain valid? We offer three guidelines. (1) If the intent is only to obtain an estimate of an inhibition constant K_I, an equilibrium analysis of Scheme 1 will provide an accurate estimate of the thermodynamic affinity of an inhibitor for either the acylation site or the peripheral site in free AChE (*18*). (2) If a substrate under investigation essentially equilibrates with AChE during reaction, an equilibrium analysis of Scheme 1 can be applied. Many slowly reacting substrates such as organophosphates (*43*) fall into this category. (3) If, however, one is investigating ligand binding to the peripheral site with substrates that do not equilibrate with AChE, kinetic parameters can be misinterpreted with an equilibrium analysis. In particular, K_{app} and K_{SS} (eq 1) will not reflect equilibrium values, and a and b (Scheme 1) will not be relative acylation and deacylation rate constants.

APPENDIX

Scheme 4 is an extension of Scheme 2 in which all complexes involving bound peripheral site inhibitor (I) are included. Our steric blockade model postulates that peripheral site binding is unaffected by acylation site ligands (i.e., $i = 1$ and the same association rate constant k_I and the same dissociation rate constant k_{-I} characterize I binding in the EI$_P$, ESI$_P$, EAPI$_P$, EAI$_P$, and EPI$_P$ complexes) and that bound peripheral site ligand has no effect on acylation and deacylation rate constants (i.e., $a = b = 1$). Our current treatment of Scheme 5 also assumes for simplicity that product P bound to the acylation site does not alter the rate constant for deacetylation ($c = e = 1$) and that P dissociation rate constants for dissociation from the acetylated enzyme are identical to those from free enzyme ($d = f = 1$). These assumptions may require future refinement in view of reported interactions between ligands and acyl groups at the acylation site (*25*, *44*). The important feature of the steric blockade model here is that $k_{S2}/k_S = k_{-S2}/k_{-S} < 1$ and that $k_{-P2}/k_{-P} < 1$.

In Scheme 3, we proposed a more detailed model of AChE catalysis in which the first step involved the formation of an ES$_P$ complex at the peripheral site. Scheme 5 is an extension of Scheme 3 in which all other complexes

Scheme 4

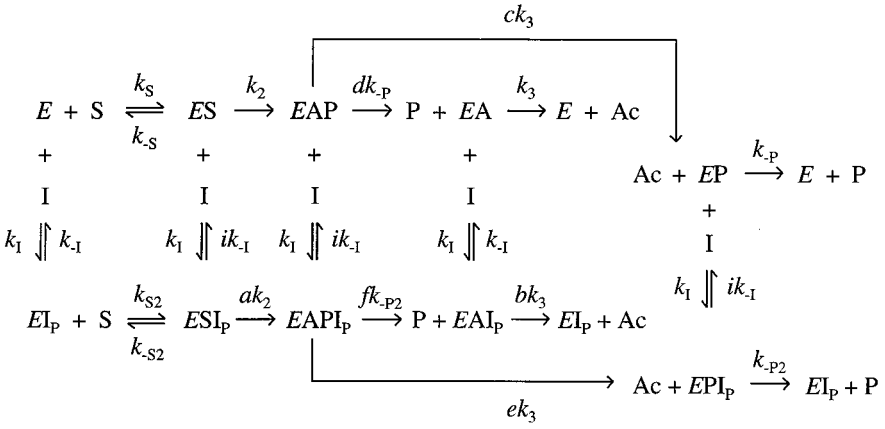

Scheme 5

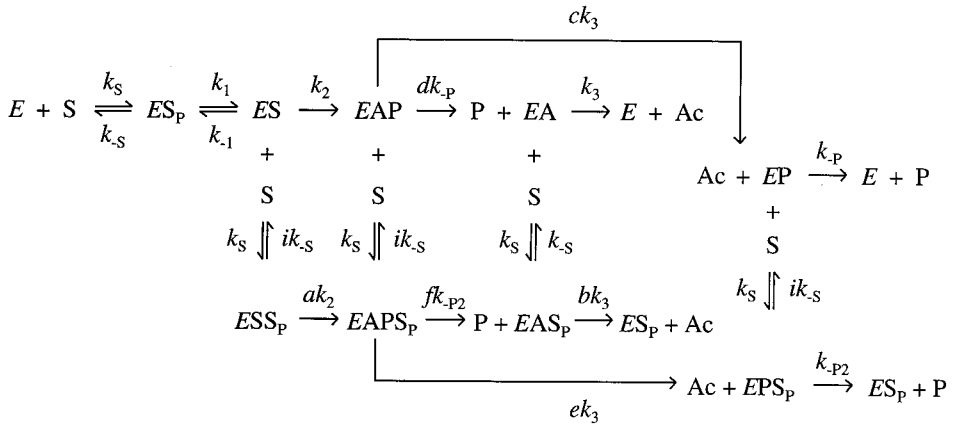

involving bound peripheral site substrate are included. As in Scheme 4, our steric blockade model postulates that $a = b = i = 1$ and that $k_{S2}/k_S = k_{-S2}/k_{-S} < 1$ and $k_{-P2}/k_{-P} < 1$, and again for simplicity, we assume that $c = d = e = f = 1$. When both S and I are present and compete for binding to the peripheral site (i.e., no enzyme species involving S_PI_P can form, such as ES_PI_P), then the five enzyme species involving I_P in Schcme 4 (EI_P, ESI_P, $EAPI_P$, EAI_P, and EPI_P) must be added to Scheme 5 to describe the complete system. While we do not show the scheme corresponding to this system, in eqs 6 and 7 we define the following combinations of enzyme species: $\sum ES_P = [ES_P] + [ESS_P] + [EAPS_P] + [EAS_P] + [EPS_P]$, $\sum EI_P = [EI_P] + [ESI_P] + [EAPI_P] + [EAI_P] + [EPI_P]$, and $\sum EX_A = [ES] + [EAP] + [EP]$. Furthermore, in the text description of eq 6, $\sum E = [E] + [EA] + \sum EX_A$. When acetylthiocholine (S) and M7A (T) are substrates simultaneously, 17 liganded species from Scheme 5 for the substrates must be considered (EA is common to both substrates) as well as six additional species representing mixed complexes (e.g., EST_P). New rate constants also are introduced by these mixed complexes (e.g., $i_{ST}k_{-T}$ is the rate constant for dissociation of T from EST_P).

ACKNOWLEDGMENT

We express our gratitude to Dr. Michel Roux at the Ecole Normale Superieure in Paris, France, for bringing the SCoP program to our attention. We also thank Dr. Abdul Fauq (Director of the Organic Synthesis Core Facility at Mayo Clinic Jacksonville) for synthesis of M7A iodide.

REFERENCES

1. Rosenberry, T. L. (1975) Acetylcholinesterase, in *Advances in Enzymology* (Meister, A., Ed.) Vol. 43, pp 103−218, John Wiley & Sons, New York.
2. Sussman, J. L., Harel, M., Frolow, F., Oefner, C., Goldman, A., Toker, L., and Silman, I. (1991) *Science 253*, 872−879.
3. Weise, C., Kreienkamp, H.-J., Raba, R., Pedak, A., Aaviksaar, A., and Hucho, F. (1990) *EMBO J. 9*, 3885−3888.
4. Schalk, I., Ehret-Sabatier, L., Bouet, F., Goeldner, M., and Hirth, C. (1992) in *Multidisciplinary Approaches to Cholinesterase Functions* (Shafferman, A., and Velan, B., Eds.) pp 117−120, Plenum Press, New York.
5. Radic, Z., Pickering, N. A., Vellom, D. C., Camp, S., and Taylor, P. (1993) *Biochemistry 32*, 12074−12084.
6. Barak, D., Kronman, C., Ordentlich, A., Ariel, N., Bromberg, A., Marcus, D., Lazar, A., Velan, B., and Shafferman, A. (1994) *J. Biol. Chem. 269*, 6296−6305.
7. Harel, M., Kleywegt, G. J., Ravelli, R. B. G., Silman, I., and Sussman, J. L. (1995) *Structure 3*, 1355−1366.
8. Bourne, Y., Taylor, P., and Marchot, P. (1995) *Cell 83*, 503−512.
9. Taylor, P., and Lappi, S. (1975) *Biochemistry 14*, 1989−1997.
10. Karlsson, E., Mbugua, P. M., and Rodriguez-Ithurralde, D. (1984) *J. Physiol. (Paris) 79*, 232−240.
11. Marchot, P., Khelif, A., Ji, Y.-H., Masnuelle, P., and Bourgis, P. E. (1993) *J. Biol. Chem. 268*, 12458−12467.
12. Nolte, H. J., Rosenberry, T. L., and Neumann, E. (1980) *Biochemistry 19*, 3705−3711.
13. Ripoll, D. R., Faerman, C. H., Axelsen, P. H., Silman, I., and Sussman, J. L. (1993) *Proc. Natl. Acad. Sci. U.S.A. 90*, 5128−5132.
14. Antosiewicz, J., McCammon, J. A., Wlodek, S. T., and Gilson, M. K. (1995) *Biochemistry 34*, 4211−4219.
15. Radic, Z., Kirchhoff, P. D., Quinn, D. M., McCammon, J. A., and Taylor, P. (1997) *J. Biol. Chem. 272*, 23265−23277.
16. Shafferman, A., Ordentlich, A., Barak, D., Kronman, C., Ber, R., Bino, T., Ariel, N., Osman, R., and Velan, B. (1994) *EMBO J. 13*, 3448−3455.
17. Barak, D., Ordentlich, A., Bromberg, A., Kronman, C., Marcus, D., Lazar, A., Ariel, N., Velan, B., and Shafferman, A. (1995) *Biochemistry 34*, 15444−15452.
18. Szegletes, T., Mallender, W. D., and Rosenberry, T. L. (1998) *Biochemistry 37*, 4206−4216.
19. Masson, P., Legrand, P., Bartels, C. F., Froment, M.-T., Schopfer, L. M., and Lockridge, O. (1997) *Biochemistry 36*, 2266−2277.
20. Rosenberry, T. L., and Scoggin, D. M. (1984) *J. Biol. Chem. 259*, 5643−5652.
21. Roberts, W. L., Kim., B. H., and Rosenberry, T. L. (1987) *Proc. Natl. Acad. Sci. U.S.A. 84*, 7817−7821.
22. Eastman, J., Wilson, E. J., Cervenansky, C., and Rosenberry, T. L. (1995) *J. Biol. Chem. 270*, 19694−19701.
23. Riddles, P. W., Blakeley, R. L., and Zerner, B. (1979) *Anal. Biochem. 94*, 75−81.
24. Ellman, G. L., Courtney, K. D., Andres, J. V., and Featherstone, R. M. (1961) *Biochem. Pharmacol. 7*, 88−95.
25. Rosenberry, T. L., and Bernhard, S. A. (1971) *Biochemistry 10*, 4114−4120.
26. Rosenberry, T. L., and Bernhard, S. A. (1972) *Biochemistry 11*, 4308−4321.
27. Haldane, J. B. S. (1930) *Enzymes*, p 84, Longmans, Green, New York.
28. Stuchbury, T., Shipton, M., Norris, R., Malthouse, J. P. G., and Brocklehurst, K. (1975) *Biochem. J. 151*, 417−432.
29. Hodge, A. S., Humphrey, D. R., and Rosenberry, T. L. (1992) *Mol. Pharmacol. 41*, 937−942.
30. Bazelyansky, M., Robey, E., and Kirsch, J. F. (1986) *Biochemistry 25*, 125−130.
31. Kasianowicz, J. J., and Bezrukov, S. M. (1995) *Biophys. J. 69*, 94−105.
32. Nachmansohn, D., and Wilson, I. B. (1951) *Adv. Enzymol. 12*, 259−339.
33. Prince, A. K. (1966) *Arch. Biochem. Biophys. 113*, 195−204.
34. Kitz, R. J., Ginsburg, S., and Wilson, I. B. (1967) *Biochem. Pharmacol. 16*, 2201−2209.
35. Krupka, R. M., and Laidler, K. J. (1961) *J. Am. Chem. Soc. 83*, 1445−1447.
36. Krupka, R. M., and Laidler, K. J. (1961) *J. Am. Chem. Soc. 83*, 1448−1454.
37. Froede, H. C., and Wilson, I. B. (1971) in *The Enzymes* (Boyer, P. D., Ed.) 3rd ed., Vol. V, pp 87−114, Academic Press, New York.
38. Zeller, E. A., and Bissegger, A. (1943) *Helv. Chim. Acta 26*, 1619−1630.
39. Aldridge, W. N., and Reiner, E. (1969) *Biochem. J. 115*, 147−162.
40. Radic, Z., Reiner, E., and Taylor, P. (1991) *Mol. Pharmacol. 39*, 98−104.
41. Hosea, N. A., Radic, Z., Tsigelny, I., Berman, H. A., Quinn, D. M., and Taylor, P. (1996) *Biochemistry 35*, 10995−11004.
42. Rosenberry, T. L. (1979) *Biophys. J. 26*, 263−290.
43. Mallender, W. D., Szegletes, T., and Rosenberry, T. L. (1999) *J. Biol. Chem.* (in press).
44. Barnett, P., and Rosenberry, T. L. (1977) *J. Biol. Chem. 252*, 7200−7206.
45. Rosenberry, T. L., Mallender, W. D., Thomas, P. J., and Szegletes, T. (1999) *Chem.-Biol. Interact.* (in press).

BI9813577